

RESEARCH

Open Access



# Strong capacity of differentiated PD-L1 CAR-modified UCB-CD34<sup>+</sup> cells and PD-L1 CAR-modified UCB-CD34<sup>+</sup>-derived NK cells in killing target cells and restoration of the anti-tumor function of PD-1-high exhausted T Cells

Farhoodeh Ghaedrahmati<sup>1</sup>, Vajihe Akbari<sup>2</sup>, Hooria Seyedhosseini-Ghaheh<sup>3</sup> and Nafiseh Esmaili<sup>1,4,5\*</sup> 

## Abstract

**Background** Using natural killer (NK) cells to treat hematopoietic and solid tumors has great promise. Despite their availability from peripheral blood and cord blood, stem cell-derived NK cells provide an “off-the-shelf” solution.

**Methods** In this study, we developed two CAR-NK cells targeting PD-L1 derived from lentiviral transduction of human umbilical cord blood (UCB)-CD34<sup>+</sup> cells and UCB-CD34<sup>+</sup>-derived NK cells. The transduction efficiencies and in vitro cytotoxic functions including degranulation, cytokine production, and cancer cell necrosis of both resultants PD-L1 CAR-NK cells were tested in vitro on two different PD-L1 low and high-expressing solid tumor cell lines.

**Results** Differentiated CAR-modified UCB-CD34<sup>+</sup> cells exhibited enhanced transduction efficiency. The expression of anti-PD-L1 CAR significantly ( $P < 0.05$ ) enhanced the cytotoxicity of differentiated CAR-modified UCB-CD34<sup>+</sup> cells and CAR-modified UCB-CD34<sup>+</sup>-derived NK cells against PD-L1 high-expressing tumor cell line. In addition, CAR-modified UCB-CD34<sup>+</sup>-derived NK cells significantly ( $P < 0.05$ ) restored the tumor-killing ability of exhausted PD-1 high T cells.

**Conclusion** Considering the more efficient transduction in stem cells and the possibility of producing CAR-NK cell products with higher yields, this approach is recommended for studies in the field of CAR-NK cells. Also, a pre-clinical study is now necessary to evaluate the safety and efficacy of these two CAR-NK cells individually and in combination with other therapeutic approaches.

**Keywords** Hematopoietic stem and progenitor cells, Differentiation, Natural killer cell, Chimeric antigen receptor

\*Correspondence:

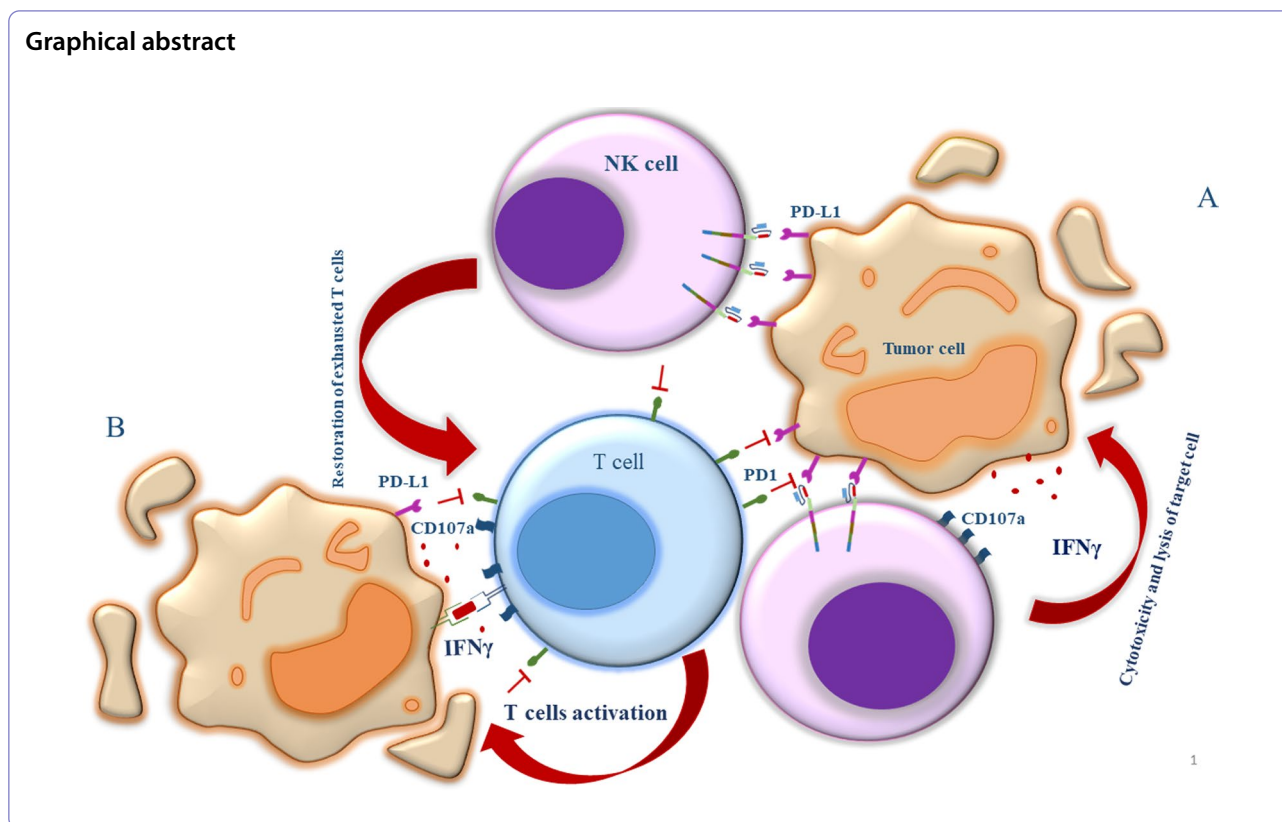
Nafiseh Esmaili

[nafesm5@gmail.com](mailto:nafesm5@gmail.com); [n\\_esmaili@med.mui.ac.ir](mailto:n_esmaili@med.mui.ac.ir)

Full list of author information is available at the end of the article



© The Author(s) 2024. **Open Access** This article is licensed under a Creative Commons Attribution-NonCommercial-NoDerivatives 4.0 International License, which permits any non-commercial use, sharing, distribution and reproduction in any medium or format, as long as you give appropriate credit to the original author(s) and the source, provide a link to the Creative Commons licence, and indicate if you modified the licensed material. You do not have permission under this licence to share adapted material derived from this article or parts of it. The images or other third party material in this article are included in the article's Creative Commons licence, unless indicated otherwise in a credit line to the material. If material is not included in the article's Creative Commons licence and your intended use is not permitted by statutory regulation or exceeds the permitted use, you will need to obtain permission directly from the copyright holder. To view a copy of this licence, visit <http://creativecommons.org/licenses/by-nc-nd/4.0/>.



## Background

Chimeric antigen receptor (CAR)-T cells have been found to be effective against hematological tumors, making adoptive cellular immunotherapy a potential clinical treatment for cancer [1]. It is important to note that autologous CAR-T therapies may be expensive and labor-intensive due to the requirement of collecting and modifying each patient's T cells, which may adversely affect patient outcomes [2]. Natural killer (NK) cells play a key role in cancer and viral infection defense [3, 4]. As an alternative to T cells, they are used in CAR-based therapies. Contrary to CAR-T cells, CAR-NK cells do not cause cytokine release syndrome (CRS) and neurotoxicity [5, 6]. The CAR-T/NK cell therapy for solid tumors, however, is hindered by an immunosuppressive tumor microenvironment (TME) [7].

A poor clinical outcome of CAR therapy is associated with up-regulation of ligands of intrinsic inhibitory receptors, such as programmed death-1 (PD-1), in the TME [8]. The PD-1 receptor is expressed on the surfaces of a wide range of immune cells, such as T cells and NK cells, and its primary ligand is programmed death-ligand 1 (PD-L1), which is upregulated on the surface of most solid tumors. The binding of PD-1 to PD-L1 leads to exhaustion and dysfunction of T/NK cells. Even though several antibodies target PD-1/

PD-L1 in the treatment of cancer, the outcome of such treatment varies from patient to patient [9–11].

Thus, it is necessary to improve the understanding of how NK cells target solid tumors and to develop modifications for NK cells that are more specific in their targeting of tumors. Consequently, previous studies have demonstrated that NK cell-mediated therapy combined with immune checkpoint inhibitors can provide greater anti-tumor efficacy [12].

Therefore, by targeting immune checkpoints such as PD-1 and PD-L1 with CAR-NK cells, we prevent the interaction between these molecules, while simultaneously identifying and attacking cancerous cells. Also, because most CAR signaling domains originate from T cell receptor signaling moieties, optimizing CAR signaling domains for NK cell signaling is important [13]. The incorporation of NK cell activating receptors such as natural cytotoxicity receptors (NCRs) and co-stimulatory receptors into CAR-NK cells may enhance their cytotoxicity.

Additionally, the acquisition of a sufficient number of effector cells with high purity and anti-cancer activity is a prerequisite for the successful application of NK cell-based treatment. Many methods have been reported for the large-scale expansion of NK cells *ex vivo* [14–16].

Leukapheresis is often used to obtain NK cells from peripheral blood mononuclear cells (PBMCs) and, more recently, from cord blood mononuclear cells (CBMCs). The cells are expanded and activated *ex vivo* with cytokines, including interleukin (IL)-2 and IL-15 before being infused into patients [17, 18]. Furthermore, CD56<sup>+</sup> NK cells can be produced by *ex vivo* differentiation of stem cells derived from various sources, such as hematopoietic stem cells (HSCs) and progenitor cells from bone marrow and umbilical cord blood (UCB), human embryonic stem cells (hESCs), and induced pluripotent stem cells (iPSCs) [19–21].

Due to their primitive stem cell characteristics and high proliferative potential, CB HSCs have been the most popular source of CD34<sup>+</sup> cells. As CB is essentially an infinite resource, this source could enable the production of large batches of quality-controlled NK cells that could be used in a variety of patients in the future [22].

In addition, mature NK cell generation from HSCs provides the opportunity to generate younger NK cells and expand specific gene-modified clones by starting with fewer numbers of previously isolated and cryopreserved initial cells, as well as the additional benefit of generating multiple batches of cells from the same donor [23–25].

Also, previous studies have shown that HSCs-derived NK cells are more homogeneous than PB NK cells and UCB-NK cells while we can generate enough NK cells from less than 250,000 input hESCs [26, 27]. Therefore, CB-HSCs facilitate large-scale production and provide a valuable source of cells for genetic engineering [28, 29].

In this study, two protocols for the production of third-generation CAR-NK cells targeting PD-L1 via viral transduction are presented, the first from differentiation of UCB-CD34<sup>+</sup> cells modified to express CAR and the second from differentiation of human UCB-CD34<sup>+</sup> cells into functional NK cells that then express CAR. The transduction efficiency and cytotoxic properties of these cells were compared *in vitro*. Also, to the best of our knowledge, our study is the first to compare the anti-cancer performance of these two types of PD-L1-specific CAR-NK cells. We also demonstrated that PD-L1 CAR-NK cells possess higher cytotoxic properties against PD-L1 high-tumor cell lines *in vitro*. Furthermore, CAR-modified UCB-CD34<sup>+</sup>-derived NK cells when co-cultured with human PBMCs stimulated with concanavalin A (ConA) restored the tumor-killing properties of PD-1 high exhausted T cells against PD-L1 low and high-tumor cell lines.

## Materials and methods

### Cell Lines and cell culture conditions

HEK 293 T packaging cells were cultured in Dulbecco's Modified Eagle Medium (DMEM) high glucose (Gibco, USA) supplemented with 10% heat-inactive fetal bovine

serum (FBS) (Gibco, USA), 100 U/ml penicillin, 100 µg/ml streptomycin, and 1 mM sodium pyruvate (Gibco, USA). MCF-7 and MDA-MB-231 cells, two breast cancer cell lines, were cultured in Roswell Park Memorial Institute (RPMI) 1640 (Gibco, USA) medium with 10% FBS, 100 U/ml penicillin, and 100 µg/ml streptomycin at 37 °C and 5% CO<sub>2</sub>.

### Isolation, expansion and differentiation of UCB-CD34<sup>+</sup> cells into NK Cells

After receiving written informed consent with regard to scientific use, fresh UCB units were taken at birth following a normal full-term delivery from the cord blood bank of the Isfahan Royan Institute (Isfahan, Iran). UCB-CD34<sup>+</sup> cells were isolated using a RosetteSep CD34 pre-enrichment cocktail followed by CD34<sup>+</sup> selection using an EasySep Human Cord Blood CD34 Positive Selection Kit II (17,896, Stemcell Technologies, Vancouver, BC, Canada). UCB-CD34<sup>+</sup> cells were used in a two-step protocol, consisting of 2 weeks of proliferation and 2 weeks of differentiation [30, 31]. Briefly, purified CD34<sup>+</sup> cells were expanded for 14 days in CellGenix<sup>®</sup> GMP SCGM (Serum-free Stem Cell Growth Medium) (Cell Genix, Freiburg, Germany) supplemented with 10% FBS, 100 U/ml penicillin, 100 µg/ml streptomycin, recombinant human stem cell growth factor (SCF; 30 ng/ml), recombinant human *fms*-like tyrosine kinase 3 ligand (FLT3L; 50 ng/ml), recombinant human IL-6 (25 ng/ml), and recombinant human thrombopoietin (TPO; 25 ng/ml) (all from BioLegend, San Diego, CA, USA). For generation and development of NK cells, from day 15 to day 28 the expanded CD34<sup>+</sup> cells were transferred to a differentiation medium containing NK MACS basal medium with 1% NK MACS supplement (Miltenyi Biotec, Bergisch Gladbach, Germany), 10% FBS, 100 U/ml penicillin, 100 µg/ml streptomycin, SCF (30 ng/ml), FLT3L (50 ng/ml), recombinant human IL-7 (50 ng/ml), recombinant human insulin-like growth factor 1 (IGF-1; 100 ng/ml), recombinant human IL-15 (50 ng/ml), and recombinant human IL-2 (500 IU/ml) (all from BioLegend) [32]. At day 28, cells were collected and the percentage of CD3<sup>-</sup>CD56<sup>+</sup> NK cells was measured by flow cytometry [33]. Also, in our unpublished article, the cytotoxic activity of these NK cells was compared with PB NK cells against K562 tumor target cells.

### Structural modeling

Single-chain variable fragment (scFv) derived from atezolizumab monoclonal antibody targeting PD-L1 and hinge from CD8α molecule were selected. We applied VH-VL orientation to CAR-NK design. The linkers used between the heavy and light chains were multimers of the pentapeptide GGGGS (glycine-serine) (15-mer (G<sub>4</sub>S)<sub>3</sub>)

or Whitlow “218” linker: GSTGSGSKPGSGEGSTKG. The structures used for homology modeling contained VH and VL variable domains with glycine-serine linker or “218” linker in addition to hinge and VH and VL variable domains without linker and hinge. Modeler v9.18 software was utilized to create the 3D structures utilizing the structure of the atezolizumab and CD8 $\alpha$  molecule (PDB IDs: 5XXY and 1CD8) as templates with the most sequence identities in the query. For the following stages, the best model with the lowest discrete optimized protein energy (DOPE) score was chosen from 1000 compared models. PROCHECK software was used to check the model’s quality.

### Molecular docking

To ensure the protein’s function will not be compromised, we examined the affinity of the scFvs for binding to PD-L1. The interaction of scFvs with PD-L1 was assessed using the HADDOCK 2.2 web server. Residues that actively contribute to protein–protein binding were selected based on a previous study (PDB ID: 5XXY) [34].

### Generation of anti-PD-L1 CAR construct

PD-L1-CAR from 5’ to 3’ comprised Xba1 site, Kozak sequence, signal peptide from CD8 $\alpha$  molecule, scFv containing VH-linker (Gly4Ser)3-VL, hinge from CD8 $\alpha$  molecule, c-Myc-tag, transmembrane region from CD28 molecule, intracellular signaling domains from 4-1BB, 2B4, and CD3 $\zeta$  molecules, stop codon, and EcoR1 site. Cop green fluorescent protein (copGFP) was used as a reporter gene. CAR construct was optimized for human codon usage synthesized by Biomatik Company (Canada) and cloned into the lentiviral vector pCDH-513B-1 containing CMV-MCS-EF1a-copGFP-T2A-Puro (System Bioscience, USA).

### Lentivirus production

The chemical-competent *E. coli* Top10 liquid containing pSPAX2 plasmids (Addgene, USA), pMD2G plasmids (Addgene, USA), or the lentiviral-vector bearing CAR structure were cultured overnight on LB solid medium containing 100  $\mu$ g/ml ampicillin. The next day, monoclonal colonies were transferred to an LB liquid medium (5 ml) supplemented with ampicillin (100  $\mu$ g/ml) for further culturing. The plasmids were extracted according to the GeneJET Plasmid Miniprep Kit instructions. Plasmids were verified by restriction enzyme digestion.

A total of  $1.2 \times 10^6$  HEK 293 T cells were cultured in a 0.2% gelatin-coated 6-well tissue culture plate. At the time of transfection, cell density was 95–99% confluent. Cells were transfected with Lipofectamine 3000 (Thermo Fisher Scientific) and DNA of lentiviral vector, gag/pol (psPAX2), and VSVG (pMD2.G) in a ratio of 2:1.5:1. Fluorescence microscopy was used to detect transfection efficiency. After 24, 48, and 72 h of transfection, the virus was harvested from the conditioned medium, centrifuged and cell debris was discarded. The supernatant was filtered using a 0.45  $\mu$ m filter unit (Millipore, United States) to remove cell debris.

### Lentivirus concentration and titration

Lentiviral particles were concentrated using PEG-8000 and ultracentrifugation. Viral titers were determined as transducing units per ml (TU/ml) by serial dilution and transduction of HEK 293 T cells in the presence of 8 mg/ml polybrene (Santa Cruz Biotechnology, USA), and then flow cytometry for GFP expression 3 days later.

### Lentiviral transduction of UCB-CD34<sup>+</sup> Cells and UCB-CD34<sup>+</sup>-derived NK cells

We used two methods for lentiviral transduction (Fig. 1). In the first one, we transduced UCB-CD34<sup>+</sup> Cells with lentivirus according to Fig. 1A. Each well of

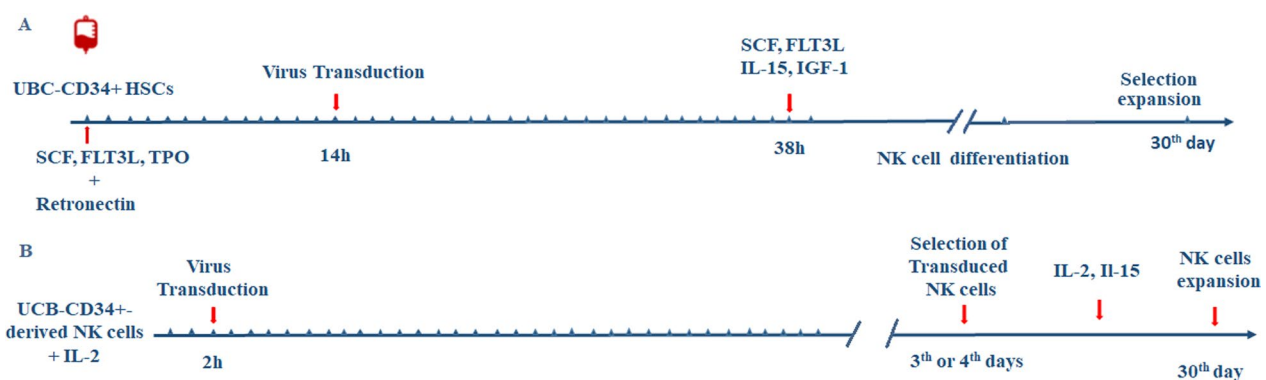


**Fig. 1** Protocol of lentiviral transduction of **A** UCB-CD34<sup>+</sup> HSCs and their differentiation into NK cells and **B** lentiviral transduction of UCB-CD34<sup>+</sup>-derived NK cells

a 12-well plate was coated with RetroNectin (3.5–5 mg/cm<sup>2</sup>) (Takara Bio), blocked with 2% FBS for 30 min, and washed with PBS. Human UCB-CD34<sup>+</sup> Cells were resuspended at 1×10<sup>6</sup> cells/ml in a transduction medium containing CellGenix<sup>®</sup> GMP SCGM supplemented with 10% FBS, 100 U/ml penicillin, 100 µg/ml streptomycin, recombinant human SCF (50 ng/ml), recombinant human FLT3L (50 ng/ml), and recombinant human TPO (50 ng/ml). On the RetroNectin-coated 12-well transduction plate, cells were added. The plate was incubated for 14 h in 5% CO<sub>2</sub> at 37 °C for pre-stimulation. After pre-stimulation, 1 ml of viral particles was added. Plate incubated for 24 h in 5% CO<sub>2</sub> at 37 °C. After 24 h cells were detached and centrifuged at 300×g for 10 min and differentiation medium containing NK MACS basal medium with 1% NK MACS supplement, 10% FBS, 100 U/ml penicillin, 100 µg/ml streptomycin, 2 mM GlutaMAX supplemented with recombinant human cytokines SCF (30 ng/ml), recombinant human FLT3L (50 ng/ml), recombinant human IL-15 (50 ng/ml) and recombinant human IGF-1 (100 ng/ml) was added. Cells were incubated at 37 °C in a humidified atmosphere with 5% CO<sub>2</sub>. CD56<sup>+</sup> NK cells appeared around day 14, and peak around day 28. During differentiation, cells were assessed by fluorescence microscopy. Surface expression of CAR was measured using a PerCP-labeled antibody to c-Myc-tag and via GFP expression. After that cells were centrifuged at 360×g for 5 min and resuspended in 1 ml NK medium containing human IL-15 (50 ng/ml), recombinant human IL-2 (500 IU/ml), and puromycin (2 µg/ml) (InvivoGen). Treatment of K562 feeder cells with MMC (50 µg/ml) (Sigma-Aldrich, USA) for 30 min was used to limit their proliferation for NK cell expansion. MMC-treated K562 feeder cells at a 1:1 (NK cell: feeder cell) ratio, IL-15 (50 ng/ml), and recombinant human IL-2 (500 IU/ml) were added to restimulate and expand the resultant CAR-NK cells. 7-AAD staining was used to determine cell viability.

In the second method, we first differentiated UCB-CD34<sup>+</sup> cells into NK cells and then transduced UCB-CD34<sup>+</sup>-derived NK cells with lentivirus according to Fig. 1B. UCB-CD34<sup>+</sup>-derived NK cells were stimulated with IL-2 for 2 h before lentiviral transduction. Each well of a 12-well plate was coated with RetroNectin (3.5–5 mg/cm<sup>2</sup>) (Takara Bio), blocked with 2% FBS for 30 min, washed with PBS, and then incubated with 1 ml viral particles in NK cell culture medium. The plate was then centrifuged at 2000×g for 1 h at 32 °C and subsequently incubated for 1 h at 37 °C. 2×10<sup>5</sup> NK cells were added and centrifuged at 1000×g for 10 min at 32 °C. After 24 h, viruses were removed by centrifuging at 360×g for 5 min, and the resulting NK cells were suspended in 1 ml NK medium with recombinant human

IL-15 (50 ng/ml) and recombinant human IL-2 (500 IU/ml). Three to four days after transduction, transduced NK cells were assessed by fluorescence microscopy and surface expression of CAR was measured using a PerCP-labeled antibody to c-Myc-tag and via GFP expression. Then cells were centrifuged at 360×g for 5 min and resuspended in 1 ml NK medium containing recombinant human IL-15 (50 ng/ml), recombinant human IL-2 (500 IU/ml), and puromycin (2 µg/ml). MMC-treated K562 feeder cells at a 1:1 (NK cell: feeder cell) ratio, recombinant human IL-15 (50 ng/ml), and recombinant human IL-2 (500 IU/ml) were added to restimulate and expand the resultant CAR-NK cells until they reached the density required for the following experiment. 7-AAD staining was used to determine cell viability.

#### **Human peripheral blood mononuclear cells (PBMCs) isolation and induction of T cell exhaustion**

Healthy young donors' PBMCs were isolated by density gradient centrifugation using 1.077 g/ml Ficoll-Histopaque (Sigma, St. Louis, MO, USA), washed twice in RPMI 1640, and resuspended in culture medium at a concentration of 10<sup>6</sup> cells/ml. To induce T cell exhaustion, ConA (Sigma-Aldrich) was added at a final concentration of 4 µg/ml for 6 days.

#### **Flow cytometry analysis**

MCF-7 and MDA-MB-231 cells were detached using 0.25% trypsin EDTA, resuspended in 100 µL of FACS buffer (1% BSA in PBS), and then incubated for 25 min with PE-conjugated anti-PD-L1 antibody (BioLegend, San Diego, CA, USA). Cell surface expression of PD-1 was assessed in ConA-stimulated PBMCs by staining with FITC-conjugated anti-human PD-1 antibody (BioLegend, San Diego, CA, USA). After washing, cells were analyzed by FACS Calibur (BD Biosciences, USA) instrument.

#### **Degranulation assay**

PD-L1 CAR-NK cells were designed to enhance their cytotoxic activity against PD-L1 positive tumor cells. Our study examined the targeting potential of PD-L1 CAR-NK cells against MCF-7 (PD-L1<sup>low</sup>) and MDA-MB-231 (PD-L1<sup>high</sup>) cells. Therefore, empty vector-transduced UCB-CD34<sup>+</sup>-derived NK cells (control), differentiated CAR-modified UCB-CD34<sup>+</sup> cells, and CAR-modified UCB-CD34<sup>+</sup>-derived NK cells were co-cultured with these two cell lines at an E:T ratio of 2:1 in triplicate wells in a U-bottom 96-well plate. Also, as part of the evaluation of the effect of PD-L1 CAR-NK cells on T cell restoration, ConA-stimulated PBMCs and ConA-stimulated PBMCs plus CAR-modified UCB-CD34<sup>+</sup>-derived NK cells were incubated with MCF-7 and MDA-MB-231

target cells at an E:T ratio 2:1 in triplicate in a U-bottom 96-well plate. CD107a staining assessed degranulation. The anti-human CD107a-APC antibody (BioLegend, San Diego, CA, USA) was added at the beginning of the co-cultures, followed by the addition of brefeldin A (1 ng/ml, BD Biosciences) one h later. After 4 h of incubation at 37 °C, cells were collected, washed, and the proportion of CD107a<sup>+</sup> cells was determined by flow cytometry.

### Cytokine assay

Culture supernatants of co-culture experiments were harvested and the concentration of IFN- $\gamma$  was determined by ELISA kits according to the manufacturer's instructions (Human IFN- $\gamma$  Mini TMB ELISA Development Kit, PeproTech, NJ, USA).

### Necrosis assay

Empty vector-transduced UCB-CD34<sup>+</sup>-derived NK cells, differentiated CAR-modified UCB-CD34<sup>+</sup> cells, and CAR-modified UCB-CD34<sup>+</sup>-derived NK cells were incubated with target MCF-7 and MDA-MB-231 cells at an E:T ratio 2:1 in triplicate wells in a U-bottom 96-well plate in 5% CO<sub>2</sub> at 37 °C for 12 h. Cells were incubated in a buffer containing propidium iodide (PI, 5  $\mu$ g/ml; Sigma-Aldrich) and were then subjected to flow cytometry analysis.

### Statistical analysis

Data presented as mean  $\pm$  SD were representative of at least three independent repeats. One-way analysis of variance (ANOVA) with post-hoc Tukey's multiple comparison test was performed to test differences among groups.  $P < 0.05$  was recognized as statistically significant. Statistical analyses were performed with GraphPad Prism 8 software (GraphPad Software Inc., San Diego, CA, USA). Flow cytometry data were analyzed using FlowJo

software V10.0.8 (FlowJo LLC., BD Biosciences, Franklin Lakes, NJ, USA).

## Results

### Validation of the 3D model's quality

Ramachandran plot statistics of the acceptable homology model (15-mer (G<sub>4</sub>S)<sub>3</sub>) with the lowest DOPE score, revealed that 89.3%, 9%, 0.8%, and 0.8% of residues are located in the most favored regions, additional allowed areas, generously allowed areas, and disallowed areas, respectively (Fig. 2).

### Molecular docking

Docking outcomes for PD-L1 interaction to each of the scFvs, HADDOCK clustered several structures, producing docking scores and energy (Table 1). Interestingly, the docking score, as well as the electrostatic and van der Waals components of the binding energy, were higher for the PD-L1/15-mer (G<sub>4</sub>S)<sub>3</sub> linker complex than for the PD-L1/GSTGSGSKPGSGEGSTKG linker complex and PD-L1/without linker complex with electrostatic and van der Waals energies playing the most important role (Table 1).

### Construction of PD-L1 CAR and preparation of CAR-NK cells

To improve the cytotoxicity of NK cells against PD-L1 positive malignant cells, a third-generation CAR with two costimulatory domains including T-cell-associated costimulatory domain 4-1BB and NK-cell-associated costimulatory domain 2B4 was constructed and inserted into a lentiviral vector system with GFP and puromycin encoding sequences (Fig. 3).

Following the transfection of HEK 293 T cells, at virus collection (72 h post-transfection), transfection efficiency was examined under a fluorescence microscope

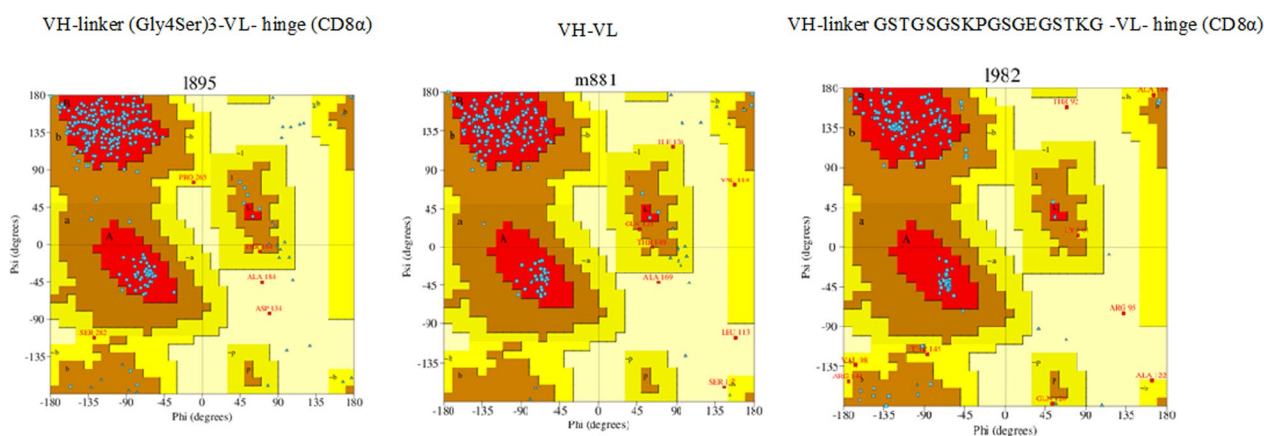


**Fig. 2** Ramachandran plots for the scFvs

**Table 1** Docking outcomes for PD-L1 interaction to each of the scFvs

Parameters	PDLI/first linker complex	PDLI/without linker complex	PDLI/second linker complex
HADDOCK score	-207.7 +/- 1.2	-186.4 +/- 1.4	-204.6 +/- 0.9
Cluster size	400	397	398
RMSD	0.4 +/- 0.3	0.4 +/- 0.3	0.5 +/- 0.3
$E_{inter}^a$	-387.8	-381	-397.8
$E_{vdw}^b$	-89.7 +/- 1.1	-84.6 +/- 3.5	-85.5 +/- 5.0
$E_{elec}^c$	-298.1 +/- 18.7	-296.4 +/- 18.3	-312.3 +/- 9.3
$E_{desolv}^d$	-60.5 +/- 3.5	-44.6 +/- 1.6	-58.4 +/- 4.2
$E_{rv}^e$	21.4 +/- 1.36	20.8 +/- 1.49	17.3 +/- 3.20
BSA <sup>f</sup>	2104.4 +/- 36.2	2071.2 +/- 8.3	2126.6 +/- 28.3
Z-score	0.0	0.0	0.0

<sup>a</sup> Intermolecular energy: sum of the van der Waals and electrostatic energies

<sup>b</sup> Van der Waals energy

<sup>c</sup> Electrostatic energy

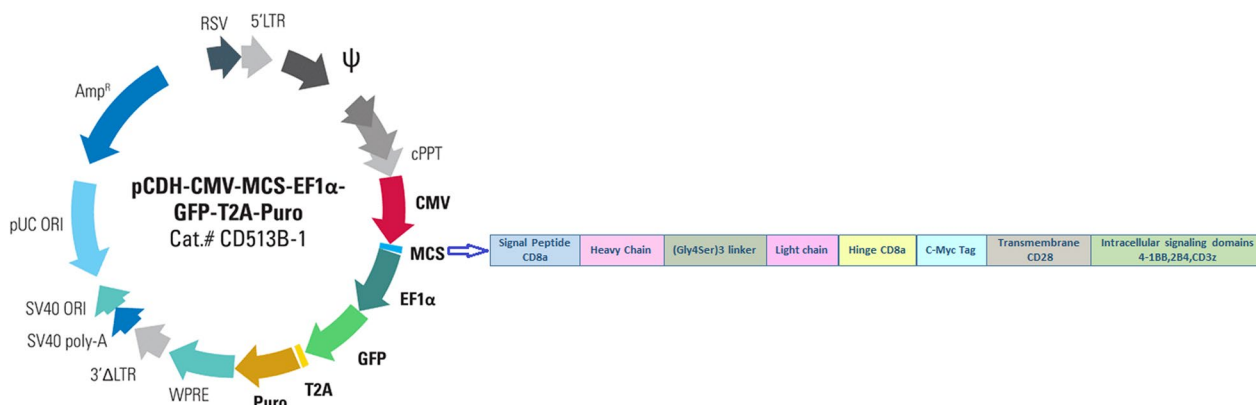
<sup>d</sup> Desolvation energy

<sup>e</sup> Restrain violation energy

<sup>f</sup> Total BSA: buried surface energy

First linker: multimers of the pentapeptide GGGGS (glycine-serine) (15-mer (G4S)3)

Second linker: Whitlow "218" linker: GSTGSGSKPGSGEGSTKG

**Fig. 3** Construction of PD-L1 CAR

and almost all HEK 293 T cells were positive for GFP (Fig. 4A). UCB-CD34<sup>+</sup> cells and UCB-CD34<sup>+</sup>-derived NK cells were transduced with the PD-L1-specific CAR to generate PD-L1 CAR-NK cells. Fluorescence microscopy displayed the successful transduction of lentiviral vector after puromycin selection and expansion in differentiated CAR-modified UCB-CD34<sup>+</sup> cells and CAR-modified UCB-CD34<sup>+</sup>-derived NK cells (Fig. 4B and C).

Transduction efficiency was significantly higher in differentiated CAR-modified UCB-CD34<sup>+</sup> cells (60–80%) (Fig. 4D–F) compared to CAR-modified UCB-CD34<sup>+</sup>-derived NK cells (20–30%) (Fig. 4G–I). Following repeated selection and expansion with puromycin (2 µg/

ml) and MMC-treated K562 feeder cells at a 1:1 (NK cell: feeder cell) ratio, respectively, the mean proportion of c-Myc-tag and GFP-positive cells exceeded 80% in the both differentiated CAR-modified UCB-CD34<sup>+</sup> cells and CAR-modified UCB-CD34<sup>+</sup>-derived NK cells. After differentiation, NK cells expanded 40–70 folds in the presence of feeder cells and cytokines.

#### Surface expression of PD-1 on ConA-stimulated human PBMCs and PD-L1 on human cancer cell lines

To evaluate the cytotoxic effect of PD-L1 CAR-NK cells, two cancer cell lines including MCF-7 with low PD-L1 expression and MDA-MB-231 with high PD-L1

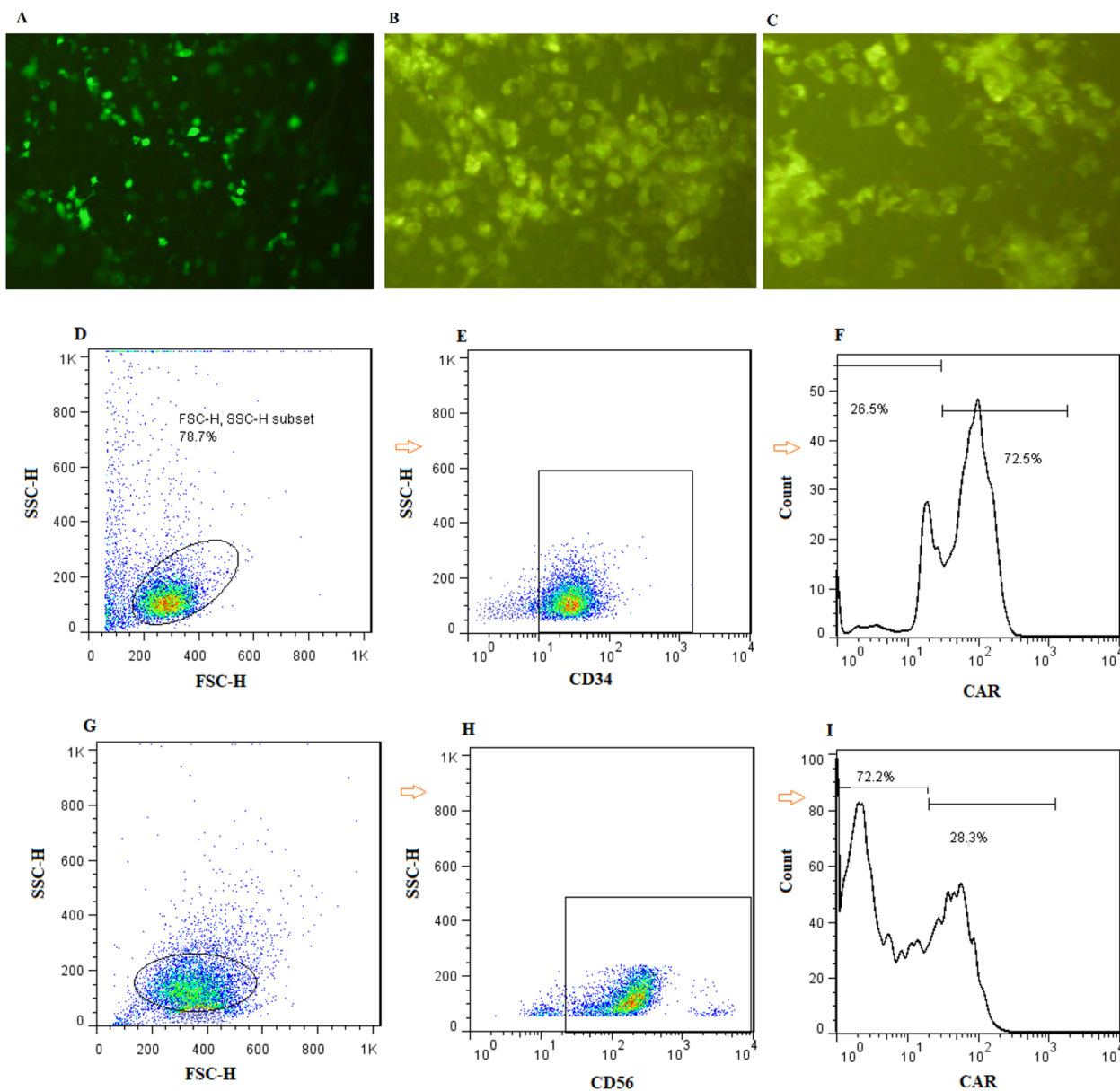


**Fig. 4** Characterization of PD-L1 CAR-NK cells. **A** Transfection efficiency in HEK 293T cells after lentivirus-mediated gene transfer using Lipofectamine 3000 reagent. Three days after transfection, the GFP in living cells was monitored using the fluorescence microscope with a 10× objective lens. It shows high GFP expression. The fluorescent microscopic image of **(B)** differentiated CAR-modified UCB-CD34<sup>+</sup> cells and **(C)** CAR-modified UCB-CD34<sup>+</sup>-derived NK cells after selection and expansion with puromycin and MMC-treated K562 feeder cells. Representative flow cytometry analysis of the expression of CAR in **D–F** differentiated CAR-modified UCB-CD34<sup>+</sup> cells and **G–I** CAR-modified UCB-CD34<sup>+</sup>-derived NK cells

expression were used and cell surface expression of PD-L1 was assessed using flow cytometry. The proportion of PD-L1 positivity was 14.5% and 93.2%, respectively (Fig. 5A and B).

To assess the cytotoxic activity of exhausted T cells before and after co-culture with CAR-modified

UCB-CD34<sup>+</sup>-derived NK cells, highly expressed PD-1 cells were prepared. Our results showed that PD-1 expression increased significantly after 6 days of stimulation with conA (4 μg/ml) from 9.83% to 55.33% (Fig. 5C).



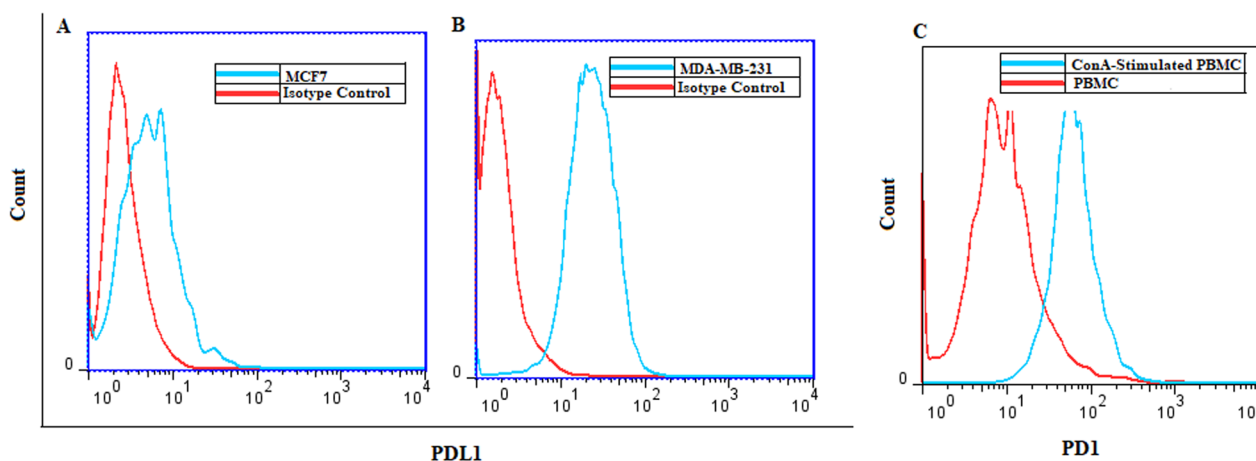


**Fig. 5** Representative flow cytometry analysis of the expression of PD-L1 and PD-1. PD-L1 expression on **A** MCF-7 and **B** MDA-MB-231 cells. **C** PD-1 expression on PBMCs after ConA stimulation for 6 days

#### Significant increase of CD107a expression by both CAR-NK cells against MDA-MB-231 cell line and co-culture of ConA-stimulated PBMCs with CAR-modified UCB-CD34<sup>+</sup>-derived NK cells against both cell lines

To determine the cytotoxicity of CAR-NK cells against MCF-7 and MDA-MB-231 cell lines, we performed the degranulation test by assessing CD107a expression levels by flow cytometry (Fig. 6A–F and G–I). UCB-CD34<sup>+</sup>-derived NK cells transduced with an empty vector (control) did not exhibit significant degranulation after 4 h of co-culture with MCF-7 and MDA-MB-231 cells (Fig. 6J and K). Incubation of MCF-7 with differentiated CAR-modified UCB-CD34<sup>+</sup> cells and CAR-modified UCB-CD34<sup>+</sup>-derived NK cells increased the effector cells' degranulation compared to control however it was not statistically significant (Fig. 6J). A significant degranulation was observed in differentiated CAR-modified UCB-CD34<sup>+</sup> cells and CAR-modified UCB-CD34<sup>+</sup>-derived NK cells incubated with MDA-MB-231 cells compared to control ( $P < 0.01$  and  $P < 0.001$ , respectively) (Fig. 6K). CAR-modified UCB-CD34<sup>+</sup>-derived NK cells induced a greater percentage of CD107a-positive cells compared to differentiated CAR-modified UCB-CD34<sup>+</sup> cells against MDA-MB-231 cell lines ( $P < 0.05$ ) (Fig. 6K). Furthermore, although CD107a expression was increased against

both MCF-7 and MDA-MB-231 cells, it was significantly higher against MDA-MB-231 cells than in MCF-7 cells (Fig. 6L). A remarkable increase in CD107a-positive cells was observed against both MCF-7 and MDA-MB-231 cells when ConA-stimulated PBMCs were co-cultured with CAR-modified UCB-CD34<sup>+</sup>-derived NK cells compared to ConA-stimulated PBMCs ( $P < 0.01$  and  $P < 0.05$ , respectively) (Fig. 6J and K). According to these findings, PD-L1 CAR-NK cells preferentially target the PD-L1 high-expressing tumor cells and restore the functionality of exhausted T cells.

#### Significant increase of IFN- $\gamma$ levels by both CAR-NK cells and co-culture of ConA-stimulated PBMCs with CAR-modified UCB-CD34<sup>+</sup>-derived NK cells against MDA-MB-231 cell line

IFN- $\gamma$ , a crucial cytokine for tumor surveillance and for stimulating T cells and macrophages, is produced primarily by NK cells and is functionally linked to their cytotoxic function. We didn't detect any significant IFN- $\gamma$  levels in the supernatant of co-culture of MCF-7 with differentiated CAR-modified UCB-CD34<sup>+</sup> cells and CAR-modified UCB-CD34<sup>+</sup>-derived NK cells compared to control (Fig. 7A). Also, we did not find significant changes in IFN- $\gamma$  levels in co-culture of MCF-7

(See figure on next page.)

**Fig. 6** Expression of CD107a. Representative flow cytometry dot plots of GFP<sup>+</sup> CD107a<sup>+</sup> population in co-culture of empty vector-transduced UCB-CD34<sup>+</sup>-derived NK cells with **A** MCF-7 and **B** MDA-MD231 cell lines as control groups, co-culture of differentiated CAR-modified UCB-CD34<sup>+</sup> cells with **C** MCF-7 and **D** MDA-MD231 cell lines, and co-culture of CAR-modified UCB-CD34<sup>+</sup>-derived NK cells with **E** MCF-7 and **F** MDA-MD231 cell lines. **G** Representative flow cytometry dot plots of co-culture of CAR-modified UCB-CD34<sup>+</sup>-derived NK cells (as GFP<sup>+</sup> cells) plus ConA-stimulated PBMCs (as GFP<sup>-</sup> cells) with target cells. GFP<sup>-</sup> cells were gated as ConA-stimulated PBMCs. Histogram plots of CD107a expression in GFP<sup>-</sup> cells population after co-culture with **H** MCF-7 and **I** MDA-MD231 cell lines. **J–L** Statistical analysis of the percentage of CD107a<sup>+</sup> positive cells. Cells were placed in culture with target MCF-7 (PD-L1<sup>low</sup>) and MDA-MB-231 (PD-L1<sup>high</sup>) cells at an E:T ratio 2:1 for 4 h. \* $P < 0.05$ , \*\* $P < 0.01$ , and \*\*\* $P < 0.001$

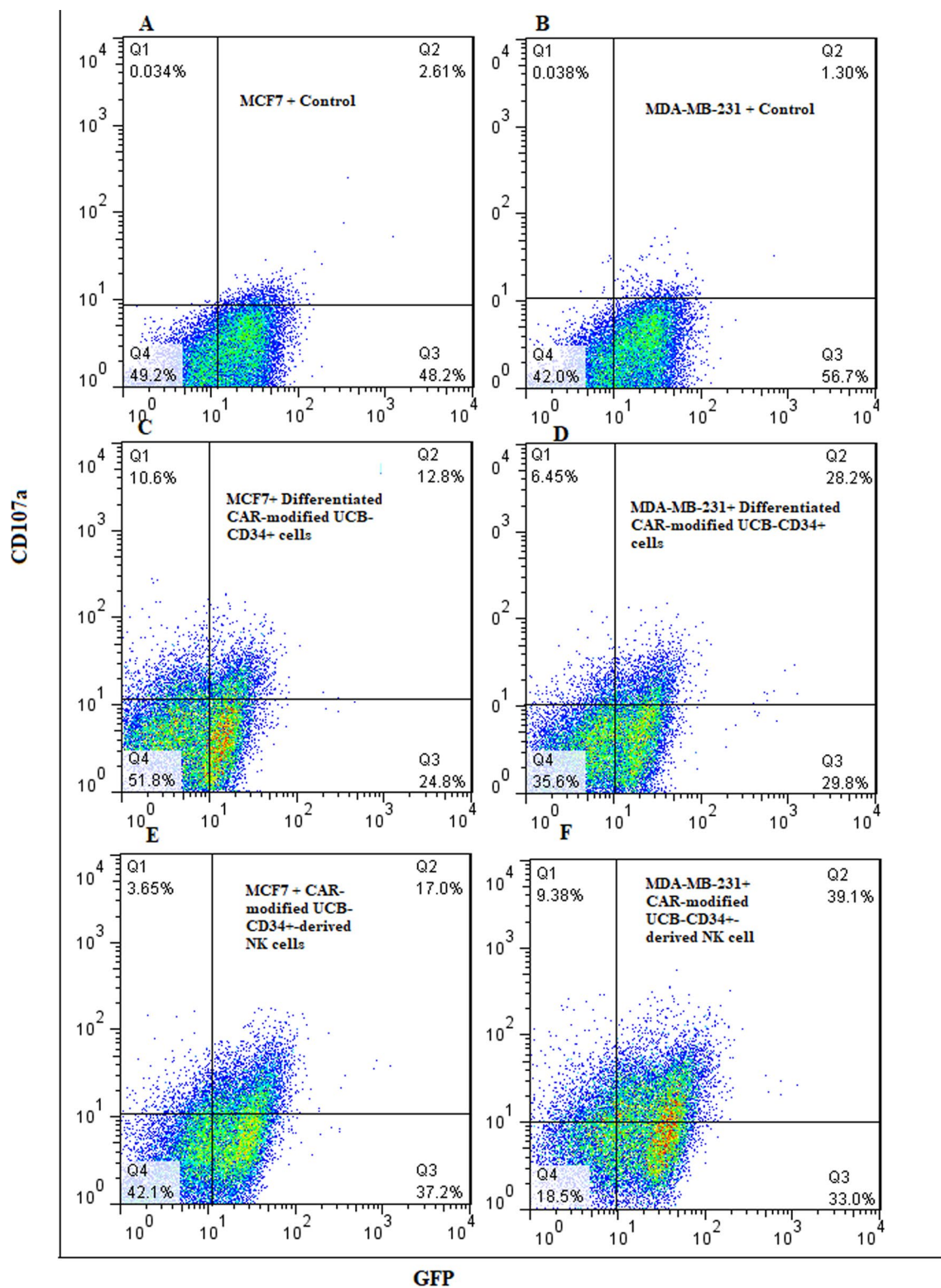


**Fig. 6** (See legend on previous page.)

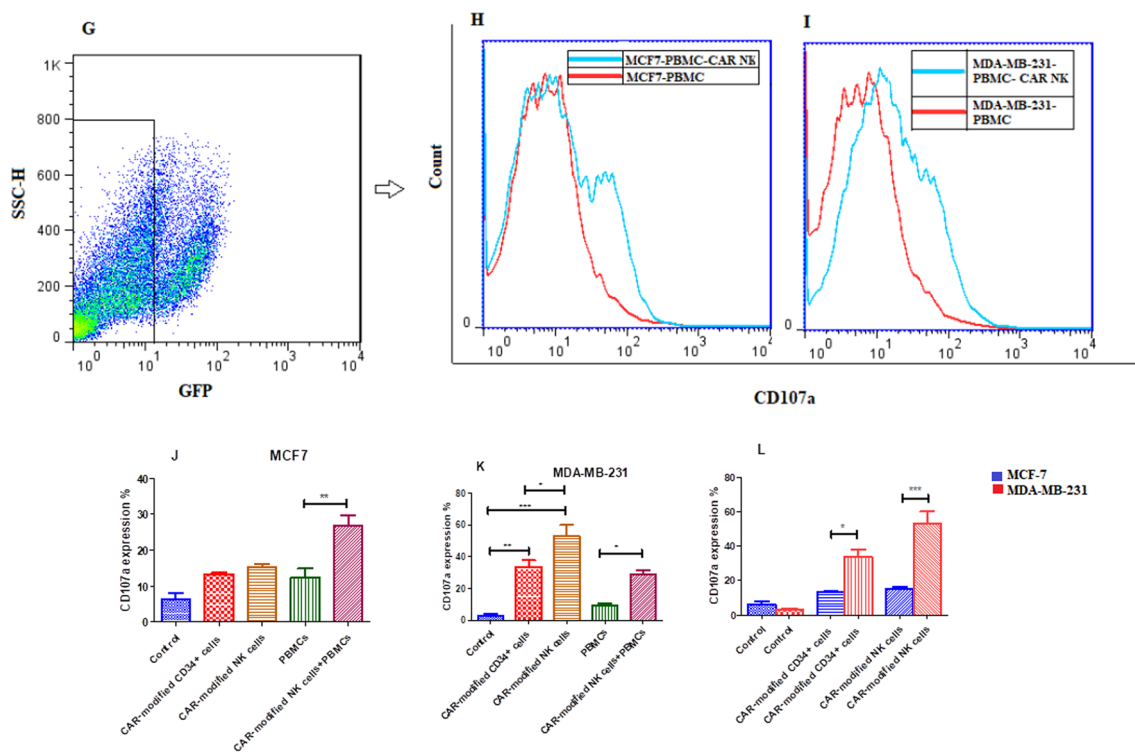
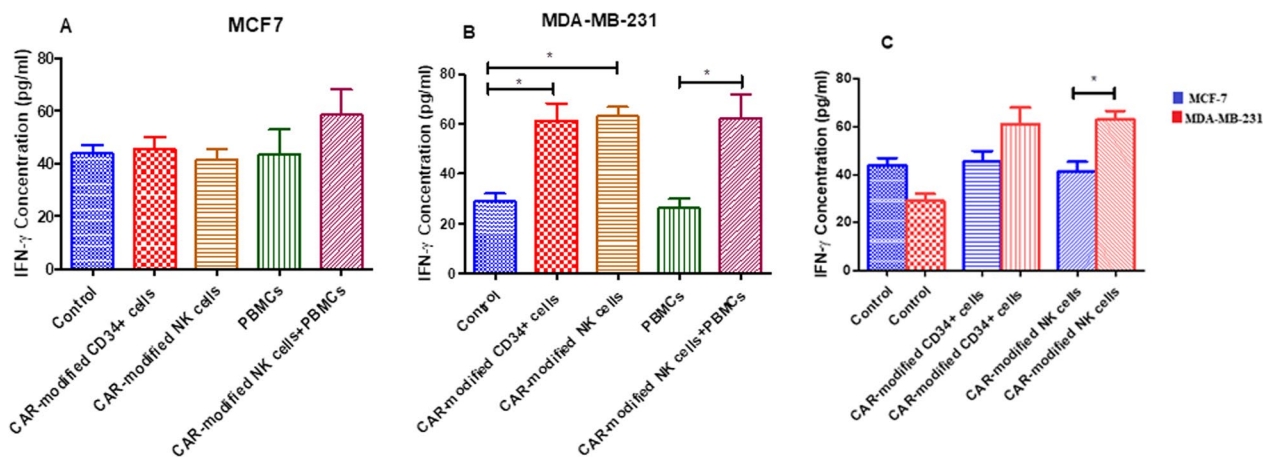


Fig. 6 continued



**Fig. 7** ELISA assay for IFN- $\gamma$  quantification. **A–C** Statistical analysis of the IFN- $\gamma$  concentration. Empty vector-transduced UCB-CD34<sup>+</sup>-derived NK cells (control), differentiated CAR-modified UCB-CD34<sup>+</sup>-derived NK cells, ConA-stimulated PBMCs, and ConA-stimulated PBMCs plus CAR-modified UCB-CD34<sup>+</sup>-derived NK cells were placed in culture with targets, including MCF-7 (PD-L1<sup>low</sup>) and MDA-MB-231 (PD-L1<sup>high</sup>) cells at an E:T ratio 2:1 for 12 h. The supernatants were collected, and an ELISA kit was used to detect the release of IFN- $\gamma$ . \* $P < 0.05$

with ConA-stimulated PBMCs plus CAR-modified UCB-CD34<sup>+</sup>-derived NK cells compared to ConA-stimulated PBMCs (Fig. 7A). The level of IFN- $\gamma$  significantly increased in the treatment of MDA-MB-231 cells with differentiated CAR-modified UCB-CD34<sup>+</sup> cells

and CAR-modified UCB-CD34<sup>+</sup>-derived NK cells compared to control ( $P < 0.05$ , for both) (Fig. 7B). Also, the cytokine released by co-culture of MDA-MB-231 cells with ConA-stimulated PBMCs plus CAR-modified UCB-CD34<sup>+</sup>-derived NK cells was significantly higher than

ConA-stimulated PBMCs ( $P < 0.05$ ) (Fig. 7B). Furthermore, the level of IFN- $\gamma$  was significantly higher against MDA-MB-231 cells than in MCF-7 cells (Fig. 7C). These data confirm a functional effect of PD-L1 CAR-NK cells mediated by increased PD-L1 expression.

#### Significant necrosis by differentiated CAR-modified UCB-CD34<sup>+</sup> cells against MCF-7 cell line and by both CAR-NK cells against MDA-MB-231 cell line

After 12 h, the cultures were harvested and target cell death by both PD-L1 CAR-NK cells was analyzed by flow cytometry, using PI for live/dead cell discrimination (Fig. 8A–F). There was no obvious killing observed in UCB-CD34<sup>+</sup>-derived NK cells transduced with an empty vector (control) (Fig. 8G and H). The necrotic effects of differentiated CAR-modified UCB-CD34<sup>+</sup> cells on MCF-7 cells were significantly increased compared to corresponding control cells ( $P < 0.01$ ) (Fig. 8G). The killing rate of MDA-MB-231 cells was increased after treatment with both differentiated CAR-modified UCB-CD34<sup>+</sup> cells and CAR-modified UCB-CD34<sup>+</sup>-derived NK cells, demonstrating the cytotoxic properties of PD-L1 CAR-NK cells ( $P < 0.001$  and  $P < 0.01$ , respectively) (Fig. 8H). The number of necrotic cells increased significantly in the treatment with differentiated CAR-modified UCB-CD34<sup>+</sup> cells as compared to CAR-modified UCB-CD34<sup>+</sup>-derived NK cells on both cell lines tested ( $P < 0.01$ , for both) (Fig. 8G and H). The percentage of necrotic cells was higher in MDA-MB-231 cells than in MCF-7 (Fig. 8I). The data presented here provide further evidence that PD-L1 CAR-NK cells preferentially target tumor cells with high levels of PD-L1.

#### Discussion

The effectiveness of immunotherapy agents that target PD-L1 has been demonstrated against various types of human cancers, with solid tumors being particularly targeted by these agents [35–37]. Besides the PD-L1 molecules that are present in many cancer cells, other cells within the TME can also hinder the anti-tumor activity of immune effector cells by producing PD-L1. The advantage of CAR-based therapies over monoclonal antibodies against PD-L1 is that they eliminate PD-L1-expressing target cells permanently within the TME, which is an obvious superiority over monoclonal antibodies that inhibit the PD-L1/PD-1 axis [38]. This study aimed to develop a third-generation CAR-NK cell targeting PD-L1 with two costimulatory domains (4-1BB and 2B4) and a CD3 $\zeta$  activation domain. Two different strategies were used to generate these cells: (1) differentiation of UCB-CD34<sup>+</sup> cells modified to express the CAR, and (2) differentiation of human UCB-CD34<sup>+</sup> cells into functional NK cells expressing the CAR. After that, we assessed the

efficiency of transduction and in vitro cytotoxic functions of both. We found that the transduction efficiency and expansion ability of UCB-CD34<sup>+</sup> cells modified to express the CAR were higher than those of NK cells derived from UCB-CD34<sup>+</sup> cells. Previous studies have shown that HSCs have a higher efficiency in transduction and expansion than CB NK cells, which is consistent with our findings [12].

In addition, in our unpublished article, our findings showed that NK cells that are derived from UCB-CD34<sup>+</sup> cells had a higher expression of activating receptors and cytotoxic activity against K562 target cells compared to PB NK cells. In this state, it is possible to obtain an ample amount of CAR-NK cells with strong cytotoxic capacity for single or multiple adoptive cell therapy. Moreover, in the present study, after differentiation, NK cells expanded 40–70 folds in the presence of feeder cells and cytokines. According to studies, different methods are used for NK cell expansion and activation, including using a cocktail of cytokines like IL-2, IL-15, and IL-18 and also irradiated feeder cells, such as Epstein–Barr virus-transformed lymphoblastoid cell lines, PBMCs, artificial antigen-presenting cells (aAPCs) or gene-modified K562 cells expressing 4-1BB ligand, IL-21 and IL-15, and other irradiated tumor cell lines [39–41].

The proliferation of NK cells with high purity has increased up to 400 folds in the presence of aAPCs, including K562-mb IL-21 cells, K562-mb IL-15, K562-mb CD86, 4-1BBL, IL-15, IL-21 [42]. Also, Lee et al. have expanded NK cells using autologous irradiated PBMCs and anti-CD16 mAb up to 5000-fold [41].

The lower level of NK cell proliferation in this study was due to the use of mitomycin-treated K562 cells as feeder cells for expansion, the capability of these cells to induce proliferation is much lower compared to the aAPCs. However, since this study was a basic experimental study to investigate the bioavailability of the PD-L1 CAR-NK cells and their function, the cells proliferated by this method provided enough cells to perform the project.

In our study, significantly higher expression of CD107a was observed in both PD-L1 CAR-NK cells after coculture with MDA-MB-231 (PD-L1<sup>high</sup>) tumor cells. Furthermore, the IFN- $\gamma$  level was increased after treatment of MDA-MB-231 tumor cells with both PD-L1 CAR-NK cells, while we did not find significant elevation in IFN- $\gamma$  level after treatment of MCF-7 (PD-L1<sup>low</sup>) tumor cells with both PD-L1 CAR-NK cells. Incubation of MCF-7 with differentiated CAR-modified UCB-CD34<sup>+</sup> cells and CAR-modified UCB-CD34<sup>+</sup>-derived NK cells resulted in an increase in effector cells' degranulation compared to control, but it wasn't statistically significant. These findings first bring to mind that MCF-7 cells, as PD-L1 low

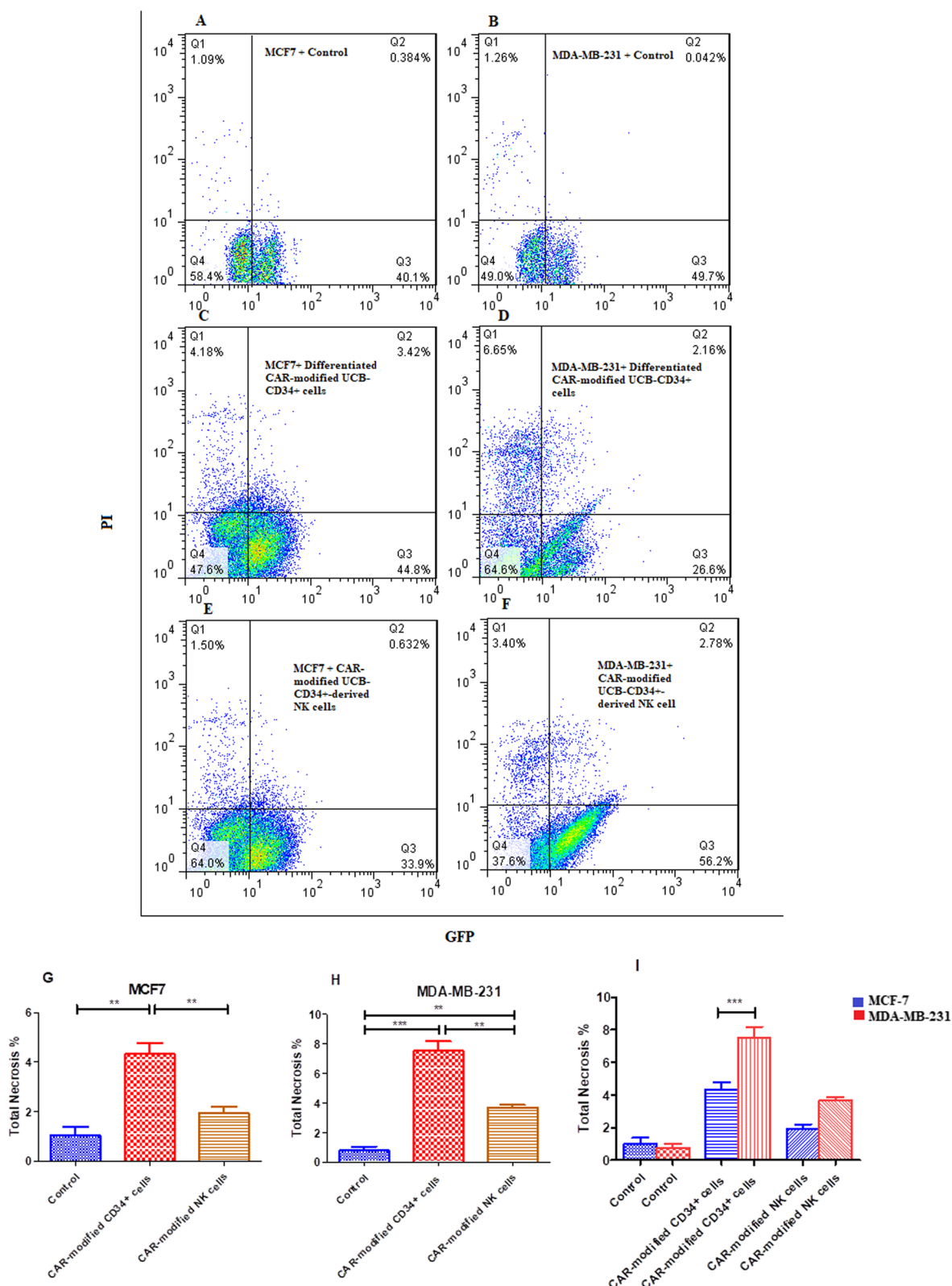


**Fig. 8** Detection of necrosis by flow cytometry. Representative flow cytometry dot plots of human MCF-7 (PD-L1<sup>low</sup>) and MDA-MB-231 (PD-L1<sup>high</sup>) cancer cell lines necrosis by **A–B** empty vector-transduced UCB-CD34<sup>+</sup>-derived NK cells, **C–D** differentiated CAR-modified UCB-CD34<sup>+</sup> cells, and **E–F** CAR-modified UCB-CD34<sup>+</sup>-derived NK cells. **G–I** Statistical analysis of the percentage of necrotic cells. Cells were placed in culture with target cells at an E:T ratio 2:1 for 12 h. \*\**p* < 0.01 and \*\*\**p* < 0.001

cells, are vulnerable to the cytotoxic function of CAR-NK cells.

On the other hand, such an effect of PD-L1 CAR-NK cells against MCF-7 cells suggests that this could be detrimental to non-malignant cells, which express low levels of PDL-1. Bajor et al. have evaluated the anti-tumor effects of PD-L1 CAR-T cells against MCF-7 (PD-L1<sup>low</sup>) and MDA-MB-231 (PD-L1<sup>high</sup>) tumor cells. Consistent with our findings, they have indicated significantly higher levels of TNF- $\alpha$ , IFN- $\gamma$ , and higher expression of CD107a after co-culture of PD-L1 CAR-T cells with MDA-MB-231 (PD-L1<sup>high</sup>) tumor cells for 4 h. They also assessed the anti-tumor effects of PD-L1 CAR-T cells against MCF-7 over a long time and showed that PD-L1 CAR-T cells significantly are capable of killing both MDA-MB-231 and MCF-7 cells [43].

Previous studies have documented that contact with effector cells and elevation in the levels of pro-inflammatory cytokines, including TNF- $\alpha$  and IFN- $\gamma$  in the environment induce PD-L1 expression on the surface of target cells, which ensues inflammation [44, 45].

Accordingly, Liu et al. have indicated an intensive cycle of inflammation and lung injury because of PD-L1 CAR-T cells, which would be triggered and cause adverse events [46]. In confirming the effect of inflammatory cytokines on the function of PD-L1 CAR-T cells, recently a clinical trial study in patients with advanced lung cancer using PD-L1 CAR-T cells (NCT03330834) showed significant side effects, which resolved by tocilizumab (anti-IL-6 receptor) and steroids treatment. However, it seems that due to the lower level of inflammatory cytokines production in NK cell responses and their shorter life span, such effects in the treatment with PD-L1 CAR-NK cells are less. Accordingly, the preliminary data from a clinical study (NCT04050709) with PD-L1 CAR-NK cells at a dose of  $2 \times 10^9$  cells intravenous (IV) twice per week, indicated its tolerability in patients without serious complications.

In the current study, we only measured the IFN- $\gamma$  levels, so the response to MCF-7 by both PD-L1 CAR-NK cells may be due to the difference in the amount of other pro-inflammatory cytokines. It is necessary to conduct more research to comprehend the responses of differentiated CAR-modified UCB-CD34<sup>+</sup> cells and CAR-modified UCB-CD34<sup>+</sup>-derived NK cells to MCF-7 cells and non-malignant PD-L1<sup>low</sup> cells. Also, studies in which the function of CAR-modified UCB-CD34<sup>+</sup> cells and CAR-modified UCB-CD34<sup>+</sup>-derived NK cells can be investigated against the target cells in which PD-L1 has been knocked down will further identify the role of anti-cancer impacts of PDL1-specific CAR-NK cells.

Furthermore, studies have revealed that the effectiveness of CAR-based approaches is influenced by PD-L1

expression and its amplification through CAR-based therapy. However, this phenomenon is an advantage in PD-L1 CAR-NK therapy due to the self-amplifying anti-tumor capability of PD-L1 CAR-NK cells [43]. Further research is necessary to determine the advantages of incorporating anti-PD-1 or anti-PD-L1 therapy or PD-L1 CAR cells into CAR-based therapies and developing dual CAR-T/NK cells [47].

Accordingly, some studies have indicated the advantages of combining PD-L1 CAR-NK cells with HER2 CAR-T cells in animal models [43, 48]. However, the antagonistic effects of the combination therapy have been observed in PD-L1 CAR-T cells when applied in addition to the mesothelin-targeting CAR-T cells [49]. In such a case, the activated mesothelin-targeting CAR-T cells probably expressed PD-L1 and were targeted by PD-L1 CAR-T cells. This effect probably can be neutralized by suppressing PD-L1 gene expression in other CAR-T/NK cells in combination with PD-L1 CAR-T/NK cells, such as knocking out the PD-L1 gene, pre-incubation of PD-L1 CAR-T/NK cells with other CAR-T/NK cells, and neutralizing of inflammatory cytokines [43, 50, 51]. However, more detailed and extensive pre-clinical studies are needed to assess the effects of treating with PD-L1 CAR-T/NK cells individually and in combination with other CAR-NK/T cells.

In response to the question of whether PD-L1 CAR-NK cells can restore the cytotoxic function of exhausted T cells expressing PD-1, we co-cultured ConA stimulated PBMCs plus PD-L1 CAR-NK cells with MCF-7 or MDA-MB-231 cell lines. According to our previous study stimulation of PBMCs with ConA for 6 days induces PD-1 and TIM-3 expression on T cells [52]. A remarkable increase in CD107a-positive cells was observed in response to MCF-7 and MDA-MB-231 cells when CAR-modified UCB-CD34<sup>+</sup>-derived NK cells were co-cultured with ConA-stimulated PBMCs compared to co-culture of ConA-stimulated PBMCs with these cell lines.

As mentioned before, the exhaustion of CAR-T/NK cells is one of the obstacles created in their anti-tumor function. Moreover, studies have shown in CD28-based CAR-T cells even in the presence of anti-PD-L1 exhaustion is happened [53]. In a clinical trial study, the treatment of 11 patients with CD19.BBz CAR-T cells showed a weak anti-tumor effect, but when they administered pembrolizumab (PD-1 antibody) in follow-up, four patients showed remission. Responder subjects experienced the restoration of exhausted CAR-T cells [54]. PD-1/PD-L1 interaction induces dephosphorylation of CD28, which results in T cell exhaustion [55].

However, signal transduction by 4-1BB stimulates cells independent of CD28, and contrary to the increase in activation-induced cell death (AICD) caused by

CD28-based CARs, 4-1BB-CD3 $\zeta$  based CARs preference for inducing memory-related genes and maintaining anti-tumor activity [56].

Cheng et al. recently designed CAR-T cells with auto-crine PD-L1 scFv and 4-1BB-containing domain against CD19 and HER2 and investigated their anti-tumor function and exhaustion in vitro and in vivo. They have indicated that in 4-1BB-based CAR-T cell exhaustion diminished by the autocrine PD-L1 scFv antibody because unlike the CD28 pathway, which is directly inhibited by PD-1/PD-L1 antibodies, the PD-1/PD-L1 blocking effect on 4-1BB signaling pathway is indirect, and this probably causes the restoration of exhausted T cells [53]. Also, consistent with our findings they have indicated in the presence of scFv PD-L1 antibody exhaustion markers of T cells, including PD-1, TIM-3, and CTLA-4 are decreased.

Therefore, the presence of the 4-1BB signaling domain in our PD-L1 CAR-NK cells was probably associated with less exhaustion in these cells, while it also caused the recovery of exhausted T cells. Our findings remind us again that combination therapy of PD-L1 CAR-NK cells containing the 4-1BB signaling domain together with other CAR-T/NK cells will have effective anti-tumor effects in addition to preventing immune cell exhaustion.

## Conclusion

According to our findings, the cytotoxic capacity of both differentiated CAR-modified UCB-CD34<sup>+</sup> cells and CAR-modified UCB-CD34<sup>+</sup>-derived NK cells was almost at the same level, and considering the more efficient transduction in stem cells and the possibility of producing CAR-NK products with a higher yield, this approach is recommended for studies in the field of CAR-NK cells. Also, our findings remind us again that combination therapy of PD-L1 CAR-NK cells containing the 4-1BB signaling domain together with other CAR-T/NK cells will have effective anti-tumor effects in addition to preventing immune cell exhaustion. Accordingly, a pre-clinical study is now necessary to evaluate the safety and efficacy of differentiated CAR-modified UCB-CD34<sup>+</sup> cells and CAR-modified UCB-CD34<sup>+</sup>-derived NK cells individually and in combination with other therapeutic approaches.

## Abbreviations

CAR	Chimeric antigen receptor
NK	Natural killer
TME	Tumor microenvironment
CRS	Cytokine release syndrome
PD-1	Programmed death-1
PD-L1	Programmed death-ligand 1
NCRs	Natural cytotoxicity receptors
PBMCs	Peripheral blood mononuclear cells
CBMCs	Cord blood mononuclear cells
HSCs	Hematopoietic stem cells

UCB	Umbilical cord blood
hESCs	Human embryonic stem cells
iPSCs	Induced pluripotent stem cells
ConA	Concanavalin A
scFv	Single-chain variable fragment
aAPCs	Artificial antigen-presenting cells
AICD	Activation-induced cell death

## Acknowledgements

The authors are grateful to the Council for Development of Regenerative Medicine and Stem Cells Technologies and the Isfahan University of Medical Sciences for financial support (Grant No. 1400182).

## Author contributions

Farhoodeh Ghaedrahmati: Conception and design, performing experiments, collection and analysis of data, and manuscript writing. Nafiseh Esmaeil: Conception and design, performing experiments, data collection, data analysis and interpretation, financial support, manuscript writing, and manuscript final approval. Vajihe Akbari: Bioinformatic assessments, study design, and final approval of manuscript. Hooria Seyedhosseini-Ghaheh: Bioinformatic assessments and interpretation and manuscript final approval.

## Availability of data and materials

Data will be available upon request.

## Declarations

### Ethics approval and consent to participate

The research project entitled "Design and construction of chimeric antigen receptor targeting PD-L1 and its expression in human umbilical cord blood stem cells-derived natural killer cells" was approved by the Research Ethics Committees of Isfahan University of Medical Sciences and Health Services Ethics Committee of the Isfahan University of Medical Sciences (code: IR.MUI.REC.1400.050) on 2021-09-29. All participants provided informed consent before enrollment in this study.

### Consent for publication

All authors hereby provide consent for the publication of the manuscript detailed above.

### Competing interests

The authors declare that they have no known competing financial interests or personal relationships that could have appeared to influence the work reported in this paper.

### Author details

<sup>1</sup>Department of Immunology, School of Medicine, Isfahan University of Medical Sciences, Isfahan 81744, Iran. <sup>2</sup>Department of Pharmaceutical Biotechnology, School of Pharmacy and Pharmaceutical Sciences, Isfahan University of Medical Sciences, Isfahan, Iran. <sup>3</sup>Nutrition and Food Security Research Center, Isfahan University of Medical Sciences, Isfahan, Iran. <sup>4</sup>Research Institute for Primordial Prevention of Non-Communicable Disease, Isfahan University of Medical Sciences, Isfahan, Iran. <sup>5</sup>Pooya Zist-Mabna Hakim Company, Poursina Hakim Institute, Isfahan, Iran.

Received: 13 May 2024 Accepted: 30 July 2024

Published online: 13 August 2024

## References

1. Maalej KM, Merhi M, Inchakalody VP, Mestiri S, Alam M, Maccalli C, et al. CAR-cell therapy in the era of solid tumor treatment: current challenges and emerging therapeutic advances. *Mol Cancer*. 2023;22(1):20.
2. Jung I-Y, Lee J. Unleashing the therapeutic potential of CAR-T cell therapy using gene-editing technologies. *Mol Cells*. 2018;41(8):717.
3. Lamers-Kok N, Panella D, Georgoudaki AM, Liu H, Ozkazanc D, Kucerova L, et al. Natural killer cells in clinical development as non-engineered engineered and combination therapies. *J Hematol Oncol*. 2022;15(1):164.

4. Myers JA, Miller JS. Exploring the NK cell platform for cancer immunotherapy. *Nat Rev Clin Oncol*. 2021;18(2):85–100.
5. Gong Y, Klein Wolterink RGJ, Wang J, Bos GMJ, Germeeraad WTV. Chimeric antigen receptor natural killer (CAR-NK) cell design and engineering for cancer therapy. *J Hematol Oncol*. 2021;14(1):73.
6. Xie G, Dong H, Liang Y, Ham JD, Rizwan R, Chen J. CAR-NK cells: A promising cellular immunotherapy for cancer. *EBioMedicine*. 2020;59: 102975.
7. Locke FL, Filosto S, Chou J, Vardhanabhuti S, Perbost R, Dreger P, et al. Impact of tumor microenvironment on efficacy of anti-CD19 CART cell therapy or chemotherapy and transplant in large B cell lymphoma. *Nat Med*. 2024;30(2):507–18.
8. Ghaedrahmati F, Esmaili N, Abbaspour M. Targeting immune checkpoints: how to use natural killer cells for fighting against solid tumors. *Cancer Commun (Lond)*. 2023;43(2):177–213.
9. Lei Q, Wang D, Sun K, Wang L, Zhang Y. Resistance mechanisms of anti-PD1/PDL1 therapy in solid tumors. *Front Cell Dev Biol*. 2020;8:672.
10. Vanhersecke L, Brunet M, Guegan JP, Rey C, Bougouin A, Cousin S, et al. Mature tertiary lymphoid structures predict immune checkpoint inhibitor efficacy in solid tumors independently of PD-L1 expression. *Nat Cancer*. 2021;2(8):794–802.
11. McGowan E, Lin Q, Ma G, Yin H, Chen S, Lin Y. PD-1 disrupted CAR-T cells in the treatment of solid tumors: promises and challenges. *Biomed Pharmacother*. 2020;121: 109625.
12. Liu WN, So WY, Harden SL, Fong SY, Wong MXY, Tan WWS, et al. Successful targeting of PD-1/PD-L1 with chimeric antigen receptor-natural killer cells and nivolumab in a humanized mouse cancer model. *Sci Adv*. 2022;8(47):eaab1187.
13. Siegler EL, Zhu Y, Wang P, Yang L. Off-the-shelf CAR-NK cells for cancer immunotherapy. *Cell Stem Cell*. 2018;23(2):160–1.
14. Fang F, Xie S, Chen M, Li Y, Yue J, Ma J, et al. Advances in NK cell production. *Cell Mol Immunol*. 2022;19(4):460–81.
15. Yao X, Matosevic S. Cryopreservation of NK and T cells without DMSO for adoptive cell-based immunotherapy. *BioDrugs*. 2021;35(5):529–45.
16. St-Denis-Bissonnette F, Cummings SE, Qiu S, Stalker A, Muradia G, Mehic J, et al. A clinically relevant large-scale biomanufacturing workflow to produce natural killer cells and natural killer cell-derived extracellular vesicles for cancer immunotherapy. *J Extracell Vesicles*. 2023;12(12): e12387.
17. Koehl U, Kalberer C, Spanholtz J, Lee D, Miller J, Cooley S, et al. Advances in clinical NK cell studies: donor selection, manufacturing and quality control. *Oncoimmunology*. 2016;5(4): e1115178.
18. Wagner J, Pfannenstiel V, Waldmann A, Bergs JW, Brill B, Huenecke S, et al. A two-phase expansion protocol combining interleukin (IL)-15 and IL-21 improves natural killer cell proliferation and cytotoxicity against rhabdomyosarcoma. *Front Immunol*. 2017;8:676.
19. Arias J, Yu J, Varshney M, Inzunza J, Nalvarte I. Hematopoietic stem cell- and induced pluripotent stem cell-derived CAR-NK cells as reliable cell-based therapy solutions. *Stem Cells Transl Med*. 2021;10(7):987–95.
20. Wen W, Chen X, Shen XY, Li HY, Zhang F, Fang FQ, et al. Enhancing cord blood stem cell-derived NK cell growth and differentiation through hyperosmosis. *Stem Cell Res Ther*. 2023;14(1):295.
21. Sun S, Wijanarko K, Liani O, Strumila K, Ng ES, Elefanti AG, et al. Lymphoid cell development from fetal hematopoietic progenitors and human pluripotent stem cells. *Immunol Rev*. 2023;315(1):154–70.
22. Shi PA, Luchsinger LL, Grealley JM, Delaney CS. Umbilical cord blood: an undervalued and underutilized resource in allogeneic hematopoietic stem cell transplant and novel cell therapy applications. *Curr Opin Hematol*. 2022;29(6):317–26.
23. Poirier N, Paquin V, Leclerc S, Lisi V, Marmolejo C, Affia H, et al. Therapeutic Inducers of Natural Killer cell Killing (ThINKK): preclinical assessment of safety and efficacy in allogeneic hematopoietic stem cell transplant settings. *J Immunother Cancer*. 2024;12(5):e008435.
24. Dege C, Fegan KH, Creamer JP, Berrien-Elliott MM, Luff SA, Kim D, et al. Potently cytotoxic natural killer cells initially emerge from erythromyeloid progenitors during mammalian development. *Dev Cell*. 2020;53(2):229–39 e7.
25. Stabile H, Fionda C, Santoni A, Gismondi A. Impact of bone marrow-derived signals on NK cell development and functional maturation. *Cytokine Growth Factor Rev*. 2018;42:13–9.
26. Knorr DA, Ni Z, Hermanson D, Hexum MK, Bendzick L, Cooper LJ, et al. Clinical-scale derivation of natural killer cells from human pluripotent stem cells for cancer therapy. *Stem Cells Transl Med*. 2013;2(4):274–83.
27. Zhang L, Liu M, Yang S, Wang J, Feng X, Han Z. Natural killer cells: of-the-shelf cytotherapy for cancer immunosurveillance. *Am J Cancer Res*. 2021;11(4):1770–91.
28. Zhu H, Kaufman DS. An improved method to produce clinical-scale natural killer cells from human pluripotent stem cells. *Methods Mol Biol*. 2019;2048:107–19.
29. Boiers C, Carrelha J, Lutteropp M, Luc S, Green JC, Azzoni E, et al. Lymphomyeloid contribution of an immune-restricted progenitor emerging prior to definitive hematopoietic stem cells. *Cell Stem Cell*. 2013;13(5):535–48.
30. Rafat A, Dizaji Asl K, Mazloumi Z, Samadirad B, Ashrafiyanbonab F, Farahzadi R, et al. Bone marrow CD34 positive cells may be suitable for collection after death. *Transfus Apher Sci*. 2022;61(6): 103452.
31. Rafat A, Dizaji Asl K, Mazloumi Z, Movassaghpour AA, Talebi M, Shانهbandi D, et al. Telomerase inhibition on acute myeloid leukemia stem cell induced apoptosis with both intrinsic and extrinsic pathways. *Life Sci*. 2022;295: 120402.
32. Farahzadi R, Valipour B, Anakok OF, Fathi E, Montazersaheb S. The effects of encapsulation on NK cell differentiation potency of C-kit+ hematopoietic stem cells via identifying cytokine profiles. *Transpl Immunol*. 2023;77: 101797.
33. Fathi E, Kholosi Pashutan M, Farahzadi R, Nozad CH. L-carnitine in a certain concentration increases expression of cell surface marker CD34 and apoptosis in the rat bone marrow CD34(+) hematopoietic stem cells. *Iran J Vet Res*. 2021;22(4):264–71.
34. Zhang F, Qi X, Wang X, Wei D, Wu J, Feng L, et al. Structural basis of the therapeutic anti-PD-L1 antibody atezolizumab. *Oncotarget*. 2017;8(52):90215.
35. Ribas A. Adaptive immune resistance: how cancer protects from immune attack. *Cancer Discov*. 2015;5(9):915–9.
36. Marhelava K, Pilch Z, Bajor M, Graczyk-Jarzynka A, Zagodzón R. Targeting negative and positive immune checkpoints with monoclonal antibodies in therapy of cancer. *Cancers*. 2019;11(11):1756.
37. Jiao Z, Zhang J. Interplay between inflammasomes and PD-1/PD-L1 and their implications in cancer immunotherapy. *Carcinogenesis*. 2023;44(12):795–808.
38. Lee YJ, Lee JB, Ha S-J, Kim HR. Clinical perspectives to overcome acquired resistance to anti-programmed death-1 and anti-programmed death ligand-1 therapy in non-small cell lung cancer. *Mol Cells*. 2021;44(5):363.
39. Perez-Martinez A, Fernandez L, Valentin J, Martinez-Romera I, Corral MD, Ramirez M, et al. A phase I/II trial of interleukin-15-stimulated natural killer cell infusion after haplo-identical stem cell transplantation for pediatric refractory solid tumors. *Cytotherapy*. 2015;17(11):1594–603.
40. Cella M, Otero K, Colonna M. Expansion of human NK-22 cells with IL-7, IL-2, and IL-1beta reveals intrinsic functional plasticity. *Proc Natl Acad Sci U S A*. 2010;107(24):10961–6.
41. Lee HR, Son CH, Koh EK, Bae JH, Kang CD, Yang K, et al. Expansion of cytotoxic natural killer cells using irradiated autologous peripheral blood mononuclear cells and anti-CD16 antibody. *Sci Rep*. 2017;7(1):11075.
42. Dobson LJ, Saunderson SC, Smith-Bell SW, McLellan AD. Sleeping Beauty kit sets provide rapid and accessible generation of artificial antigen-presenting cells for natural killer cell expansion. *Immunol Cell Biol*. 2023;101(9):847–56.
43. Bajor M, Graczyk-Jarzynka A, Marhelava K, Burdzinska A, Muchowicz A, Goral A, et al. PD-L1 CAR effector cells induce self-amplifying cytotoxic effects against target cells. *J Immunother Cancer*. 2022;10(1):e002500.
44. Ribas A. Adaptive immune resistance: how cancer protects from immune attack. *Cancer Discov*. 2015;5(9):915–9.
45. Liu G, Zhang Q, Li D, Zhang L, Gu Z, Liu J, et al. PD-1 silencing improves anti-tumor activities of human mesothelin-targeted CART cells. *Hum Immunol*. 2021;82(2):130–8.
46. Liu H, Ma Y, Yang C, Xia S, Pan Q, Zhao H, et al. Severe delayed pulmonary toxicity following PD-L1-specific CAR-T cell therapy for non-small cell lung cancer. *Clin Transl Immunology*. 2020;9(10): e1154.
47. Kostic P, Maher J, Arnold JN. Perspectives on chimeric antigen receptor T-cell immunotherapy for solid tumors. *Front Immunol*. 2018;9:11104.
48. Fabian KP, Padgett MR, Donahue RN, Solocinski K, Robbins Y, Allen CT, et al. PD-L1 targeting high-affinity NK (t-haNK) cells induce direct antitumor effects and target suppressive MDSC populations. *J Immunother Cancer*. 2020;8(1):e000450.



49. Qin L, Zhao R, Chen D, Wei X, Wu Q, Long Y, et al. Chimeric antigen receptor T cells targeting PD-L1 suppress tumor growth. *Biomark Res.* 2020;8:19.
50. Chaganty BKR, Qiu S, Gest A, Lu Y, Ivan C, Calin GA, et al. Trastuzumab upregulates PD-L1 as a potential mechanism of trastuzumab resistance through engagement of immune effector cells and stimulation of IFN gamma secretion. *Cancer Lett.* 2018;430:47–56.
51. Vivekanandhan S, Knutson KL. Resistance to Trastuzumab. *Cancers (Basel).* 2022;14(20):5115.
52. Mohammadzadeh S, Andalib A, Khanahmad H, Esmail N. Human recombinant soluble PD1 can interference in T cells and Treg cells function in response to MDA-MB-231 cancer cell line. *Am J Clin Exp Immunol.* 2023;12(2):11–23.
53. Cheng K, Feng X, Chai Z, Wang Z, Liu Z, Yan Z, et al. 4–1BB-based CAR T cells effectively reverse exhaustion and enhance the anti-tumor immune response through autocrine PD-L1 scFv antibody. *Int J Mol Sci.* 2023;24(4):4197.
54. Chong EA, Alanio C, Svoboda J, Nasta SD, Landsburg DJ, Lacey SF, et al. Pembrolizumab for B-cell lymphomas relapsing after or refractory to CD19-directed CAR T-cell therapy. *Blood.* 2022;139(7):1026–38.
55. Cherkassky L, Morello A, Villena-Vargas J, Feng Y, Dimitrov DS, Jones DR, et al. Human CART cells with cell-intrinsic PD-1 checkpoint blockade resist tumor-mediated inhibition. *J Clin Invest.* 2016;126(8):3130–44.
56. Zhang B, Yang M, Zhang W, Liu N, Wang D, Jing L, et al. Chimeric antigen receptor-based natural killer cell immunotherapy in cancer: from bench to bedside. *Cell Death Dis.* 2024;15(1):50.

### **Publisher's Note**

Springer Nature remains neutral with regard to jurisdictional claims in published maps and institutional affiliations.